SUPPLEMENTAL MATERIAL

TRPV4-Mediated Calcium-Influx into Human Bronchial Epithelia upon Exposure to Diesel Exhaust Particles

Jinju Li[1], Patrick Kanju[1,2,*], Michael Patterson[2,*], Wei-Leong Chew[2], Seung-Hyun Cho[3], Ian Gilmour[3], Tim Oliver[4], Ryohei Yasuda[2,5], Andrew Ghio[6], Sidney A. Simon[2], Wolfgang Liedtke[1,2]

Duke University, Departments of Medicine, Neurobiology, Cell Biology
Durham, NC 27710 USA

Howard Hughes Medical Institute, Chevy Chase, MD USA

US Environmental Protection Agency, Research Triangle Park and Chapel Hill, NC, USA

* equal contribution

affiliations:
1: Duke University Department of Medicine, Durham, NC
2: Duke University Department of Neurobiology, Durham, NC
3: EPA, Research Triangle Park, NC
4: Duke University Department of Cell Biology, Durham, NC
5: Howard Hughes Medical Institute, Chevy Chase, MD
6: EPA, Chapel Hill, NC

correspondence to
Dr. Wolfgang Liedtke, Duke University Center for Translational Neuroscience, Box 2900, Durham NC 27710, USA; tel. +1-919-684-0058, fax +1-684-6514
e-mail: wolfgang@neuro.duke.edu; www.liedtkelab.org

TOC

SUPPLEMENTARY MATERIALS AND METHODS

Many of the methods used in this study were described previously (Li et al. 2009).

Cell Culture and DEP Particles

BEAS-2B human airway epithelial cells

BEAS-2B cells are SV-40 transformed immortalized human bronchial epithelial cells that were obtained from ATCC (Rockville, MD). They were used between passages 65 to 85. Cells were maintained in keratinocyte growth media (KGM, Lonza, CA). For imaging studies, 1 day prior to use, cells were plated at a density of $1x10^5$ cells/mL on 12-mm-diameter poly-D-lysine coated glass coverslips (Carolina Biological Supply, Burlington, NC).

Primary human bronchial epithelial cells (HBE)

All investigations with primary human cells were IRB-approved. Human bronchial epithelial cells (HBE) were obtained from healthy, non-smoking adult volunteers by cytologic brushing of the airways during bronchoscopy (Ghio and Cohen 2005). These cells were expanded to passage 3 in bronchial epithelial growth medium (BEGM; Clonetics, San Diego, CA), plated on collagen-coated filters with a 0.4-μm pore size (Trans-CLR, Costar, Cambridge, MA) at a density of $1x10^5$ cells/filter and inserted into 12-well culture plates. The cells were maintained in a 1:1 mixture of BEGM and DMEM-H with singlequot supplements, bovine pituitary extracts (13 mg/mL), bovine serum albumin (1.5 mg/mL), and nystatin (20 units/mL) in 0.5 mL in the apical chamber and 1.5 mL in the basal chamber. Fresh medium was provided every 48 hours. Media was removed

from the apical chamber at least 24 hours prior to use to create an air-liquid interface. For measurement of secreted mediators (e.g. MMP-1), media was sampled from the lower compartment. Cells were used 3-5 days after passage 3 for acute HBE cells, that did not yet display a terminally-differentiated phenotype, and 14-21 days after passage 3 for chronic HBE cells. Chronic HBE cells had a polarized phenotype including ciliation. As compared to BEAS-2B permanent cells, primary HBE cells maintained in air-liquid-interface culture devices had a 5-10x increased cell density (Li et al. 2009).

Diesel exhaust particles (DEP), Organic extract (OE) and carbon control particles (P90)

A detailed description of the DEPs that were generated at the US EPA main campus in Research Triangle Park, NC, was given previously (Li et al. 2009).

For generation of OE (Gilmour et al. 2007), organics in 2g of DEP were extracted with methylene chloride using a Soxhlet extractor. Under nitrogen-flow, the methylene chloride in the extract was evaporated, and then the concentrated residual organics were subsequently solvent-exchanged with dimethylsulfoxide (DMSO). Using a methylene-chloride extraction method, the percent extractable organic material (by weight) in DEP, was determined at 25.9%. The concentration of organics in the final stock was adjusted to 10 mg/mL in DMSO.

Degussa Printex 90 carbon nanospheres (“P90”) were the generous gift of Dr. Winfried Moeller, GSF National Research Center for Environment and Health, Neuherberg/Munich, Germany. Investigations at the GSF have demonstrated that P90 were relatively pure carbon particles, i.e. very low in organic contamination and also in metals and water-soluble contamination. Because

of this feature, also because they have a similar size as the DEP carbonaceous core, and because of their demonstrated lack of effect on lung alveolar cells they were used as control particles (Fig. S1).

DEP and P90 were applied in concentration of 100 µg/mL, a concentration in the realistic aerogenic exposure range, and subjected to rigorous vortexing (300") before application. To match a concentration of 100 µg/mL DEP, OE dissolved in DMSO, was diluted 1:500, resulting in a concentration of 20µg/mL. In order to absorb OE to inert carbon particles, OE was incubated with P90 for 1h at room temperature, and then washed 3 times. Pelleted OE-loaded P90 were used to determine whether they can mimic the activity of DEP.

Chemicals: We used the following compounds: Pertussis toxin (inhibitor $G_{i/o}$; Sigma), U73122 (PLC inhibitor; Tocris), LY294002, PI828 (PI3-kinase inhibitors; Tocris), 4α-PDD (TRPV4 activator; Tocris), GSK205 (TRPV4 blocker; Duke Chemical Synthesis Facility (Phan et al. 2009)), Ruthenium Red (TRP(V) blocker; Tocris), $GdCl_3$ (SOCE-inhibitor at 5µM; Sigma), Thapsigargin (Ca^{++}-store depletion; Tocris), GM1489, Z-PDLDA-NHOH (pan-MMP inhibitors; Endogen), W-7 (Calmodulin inhibitor, Sigma).

Transfection of *MMP-1*-promoter reporter constructs

The *MMP-1* reporter plasmids of -4400, -3292, -2942, -2002 used in this study harbored the firefly luciferase reporter gene under the transcriptional control of the human *MMP-1* promoter.

1 µg of DNA from promoter constructs was transiently transfected using ExGen 500 (Fermentas, Glen Burnie, MD) into BEAS-2B cells in 24-well plates. As evidenced by fluorescent reporters, the transfection efficiency was >70% (results not shown). Following transfection, cells were washed and exposed to DEP, P90 and/or chemical modulators for 24h. Cell lysates were generated using 25 mM Tris (pH 7.8), 2 mM EDTA, 10% glycerol, 2 mM DTT, 1% Triton X-100, for assaying of luciferase in a 96-well-plate luminometer (Veritas Microplate Luminometer, Turner Biosystems, Mountain View, CA), using the Dual Luciferase Reporter Assay System (Promega, Thousand Oaks, CA). All transfections were carried out at least in triplicate, most in quadruplicate, and cells were co-transfected with a promoter-less Renilla luciferase construct to control for transfection efficiency as well as for cell viability. Reporter assays experiments were repeated at least once. Data were normalized for Renilla activity to account for transfection efficiency and cell viability.

Ca^{++}-imaging

Changes in intracellular Ca^{++} concentration were determined using Fura-2-AM-based ratiometric Ca^{++}-imaging. In brief, cells were incubated, for 30 min at room temperature (25^{o}C) with 2µM fura-2 acetoxy-methylester (Fura-2-AM) in external solution (in mM): 134 NaCl, 6 KCl, 1.2 $MgCl_2$, 2 $CaCl_2$, 10 glucose, 10 HEPES (pH 7.4). A Ca^{++}-free buffer solution was prepared by omitting $CaCl_2$. After exposure to Fura-2-AM, cells were washed and allowed to de-esterify for 30 min. The Fura-2-AM -loaded cells were then placed in a perfusion chamber mounted on the stage of an Olympus BX60 upright microscope that was equipped with an image acquisition and analysis system appropriate for Fura-2 Ca^{++}-imaging as described previously (Li et al. 2009).

Cells were imaged using a 40x/0.8 numerical aperture water immersion objective (Olympus). Fluorescence changes of individual cells were determined at 340 and 380 nm excitation and 510 nm emission, and the time-course of the ratio of fluorescent signals (F340/F380) was sampled at 0.5Hz using RATIOTOOL (ISEE, Raleigh, NC) and stored on the hard disk of a Macintosh computer. All Ca^{++}-imaging experiments were carried out at room temperature (~24^{o}C). Results were converted to $\Delta R/R_0$ where ΔR is the difference in fluorescence ratio (F340nm/F380nm) vs. R_0, the fluorescence ratio before stimulus application.

DEP was applied to cells at a concentration of 100 µg/mL. OE was applied at 20µg/mL (1:500 dilution of stock), taking into account all cells for image acquisition. In case cells were transfected with DNA constructs, then RFP-expression of the respective fusion proteins was used to select cells for Ca^{++} measurements.

PI3-kinase FRET imaging

To investigate how PI3-kinase (PI3-K) activity changes in BEAS-2B cells in response to DEP, we used a FRET sensor to measure the formation of PIP3 at the level of the plasma membrane. Our FRET sensor consisted of membrane targeted eGFP as a donor, and mCherry-tagged pleckstrin homology domain of Bruton's tyrosine kinase (mCh-Btk) as an acceptor. When PIP3 levels are low, mCh-Btk will be cytosolic; when PIP3 levels increase, mCh-Btk will translocate to the plasma membrane, causing FRET. To quantify FRET, we measured the fluorescence lifetime of eGFP using 2-photon fluorescence lifetime imaging (Yasuda et al. 2004). The imaging solution was identical to that used for Ca^{++} imaging. To verify that our sensor measured PI3K,

we applied PI3K inhibitors (10μM LY294002, 50μM PI828). All experiments were conducted at room temperature.

Immunocytochemistry

For double staining using the immunofluorescence method, Primary HBE cells, which grow on the transwell plates were washed 3 times with PBS and fixed with 4% PFA for 20 min on ice. The slides then were incubated with PBS containing 0.3% Triton X-100 (PBS-Triton) and 10% normal goat serum. The sections were then incubated for 24 h at 4˚C with rabbit polyclonal anti human PLCß3, (Abcam, MA), mouse monoclonal PAR-2 antibody (Santa Cruz, CA), mouse monoclonal acetylated a-tubulin (Sigma-Aldrich, MO), rabbit polyclonal anti-human TRPV4 antibody (Alomone, Jerusalem, Israel), all of them are diluted in 0.3% PBS-Triton with 3% goat serum. After washing, sections were incubated with Alexa Fluor 488-conjugated goat anti-mouse IgG (H+L), Alexa Fluor 594-conjugated goat anti-rabbit IgG (H+L) (Invitrogen Corporation, CA). Control experiments were conducted using identical amounts of non-specific isotype mouse antibody and rabbit antibody.

For confocal microscopy, images were collected at a minimum resolution of 1024x1024 px with a 63x (oil), 1.4NA Plan-Apochromat lens on a Zeiss LSM710 confocal imaging platform (Carl Zeiss, Thornwood, NY). Z-stacks were collected and viewed in order to increase detail of the X-Z profile, line scans were made with over-sampling of Z-lines (better than 0.35 μm XZ spacing) in order to visualize the finest details and dimensions of cell profiles along the optical axis. 3D-volumes were also viewed in Zen software (Carl Zeiss, Thornwood, NY) at an XYZ pixel proportionality of 1:1:1 in order to better appreciate dimensions and morphology of ciliated cells.

Co-immunoprecipitation and Western blotting

For Co-IP experiments, BEAS-2B cells were grown to 85% confluence. Cells (10^6) were harvested in lysis buffer (PBS containing 1% NP40, 1mM DTT and protease inhibitor), and exactly 100µg protein was incubated with either rabbit anti-PLC-ß3 or rabbit anti-TRPV4, or mouse monoclonal anti PAR-2 overnight at 4^{o}C. 15µL of Protein A/G-Sepharose was then added to the lysates and incubated at 4^{o}C for 4h. Beads were washed with PBS and complexes were evaluated by western blotting using TRPV4, PAR-2, or Calmodulin antibodies. Normal rabbit antiserum or mouse isotype-specific IgG was used as control.

Western blotting was performed using standard methods. Briefly, BEAS-2B cells were lysed with RIPA buffer, separated on an 10% SDS polyacrylamide gel, and then transferred to PVDF filters (0.45 µm pore; Millipore, Amherst MA) by semi-dry blot using Tris-glycine/20% methanol transfer buffer. Blotted proteins were immuno-detected using a two-step antibody-mediated chemoluminescence assay, employing specific antibodies against TRPV4 (LifeSpan BioSciences, Inc. WA), PLCß3, PAR-2 and Calmodulin, and secondary peroxidase-coupled antibodies (Jackson Immunoresearch, PA).

Phosphorylated ERK trafficking assay was done as described before (Li et al. 2009). Briefly, BEAS-2B cells were stimulated either with DEP or OE and fixated with 4% paraformaldehyde at time-points 5', 10', 20' and 30'. Phosphorylated $ERK_{1/2}$ was verified by fluorescent immuno-detection as described previously, and quantified densitometrically, corrected for background, in the nuclear area using ImageJ for at least 75 cells per time-point.

ELISA Assays

MMP-1 ELISA was performed following standard protocols as described previously. RANTES and IP-10 cytokines were measured as part of a multiplex ELISA following the instructions of the manufacturer (Bio-Rad Laboratories, Hercules, CA). ELISA output was normalized for cell viability (see next). ELISA assays were conducted using quadruplicate cellular replicates, experiments conducted at least twice.

Cell viability

To assess cell viability in response to DEP, also in response to lack of extracellular Ca^{++}, live-cell dye Hoechst 33342 ((5 µg/ml) for 20 min) was used on both, BEAS-2B and primary HBE cells, after stimulus exposure for 24 hours. The cells were then stained with Hoechst 33342 (5 µg/ml, 20 min at 25°C) and photomicrographed in order to detect apoptotic nuclei. Staurosporine (500 nM) was used as positive control for induction of apoptosis.

Statistical Analysis

Mean and SEM of quantified outcome parameters after stimulation were compared to their respective controls. Group comparisons were performed using Student's t-test or ANOVA with post-hoc Scheffe test for multi-group comparison, applying a statistics program, StatPlus:mac (AnalystSoft, Vancouver, BC Canada). Minimum significance was set $p<0.05$. Minimum significance was set at $p<0.05$. Throughout the paper, * denotes $p<0.05$, ** $p<0.01$ and *** $p<0.001$.

siRNA was transfected into BEAS-2B cells following instructions of the manufacturer and previously published methods (Li et al. 2009). siRNA was directed against PAR-2, PAR-1 (Santa Cruz Biotechnology), ß-arrestins$_{1/2}$ (Dharmacon) and TPRV4 (Dharmacon). Scrambled controls were used as provided by the manufacturer (Dharmacon). Efficiency of siRNA was confirmed for PAR-2 and TRPV4 by Taqman qRT-PCR, and for ß-arrestins$_{1/2}$ and TRPV4 by Western blot. Primers and probes were purchased from Applied Biosystems specific for PAR-2, TRPV4 and ß-actin. TRPV4 specific antibody was purchased from Alomone, raised in rabbits against the C-terminal 12 amino acids. ß-arrestin antibodies were supplied generously by Dr. R. Lefkowitz, Duke University.

TRPV4 and TRPV3 dominant-negative isoforms

These were generated by isolating a truncated form of each channel (Perez et al. 2002), from 10 amino-acids N-terminal of the 5th ransmembrane domain to 10 amino-acids C-terminal of the 6th transmembrane domain. In addition, two positive-charge point mutations were generated as M680K and D680K for TRPV4 and L639K and D641K for TRPV3. Both of these constructs were C-terminally fused to monomeric RFP, and they did lead to protein expression in BEAS-2B cells and other cell lines (HEK293T, N2a), evidenced by red fluorescence. When co-transfected with TRPV4, the dominant-negative isoform fully eliminated Ca^{++} influx in response to 4α-PDD and hypotonicity.

Electrophysiological Recordings

Whole cell currents were recorded in $TRPV4_{WT}$ or in $TRPV4_{P19S}$ transfected N2A neuronal cells. Using an inverted fluorescent microscope, cells that showed appreciable expression of C-terminally RFP-tagged TRPV4 channels were selected for patching. Patch-clamp recordings were performed 12–48 h after transfection. In order to retain the internal milieu of the cells in these experiments we used perforated patch methodology. Briefly, we incorporated 240µg/mL amphotericin B in the patch pipet tip. The data was acquired at 2 kHz using an Axopatch 200B amplifier, sampled at 20 kHz using Digidata 1322A interface (Molecular Devices, Sunnyvale, CA). Recording electrodes (3-4 MΩ) were pulled from borosilicate glass capillaries using a P-80 puller (both from Sutter Instrument, Novato, CA). Patch pipettes were then filled with a solution containing (in mM): 100 K-gluconate, 5 $MgCl_2$, 0.6 EGTA, 10 Hepes, 2 Na_2ATP and 0.3 NaGTP (290 mosmol/L, pH 7.3). The bathing solution contained 125 mM NaCl, 20 mM D-glucose, 1mM $MgCl_2$, 2.5 mM KCl and 1.5 mM Hepes (300 mosmol/L, pH 7.3). Cells' membrane potential was held at 0 mV while applying voltage ramps from -100 mV to +110 mV at a frequency of 0.2Hz. After establishment of baseline, Ca^{++}-activation with 2 mM $CaCl_2$ was applied (Strotmann et al. 2003; Strotmann et al. 2010). TRPV4 channel activity was confirmed by addition of GSK205 (10µM) (Phan et al. 2009). Experiments were performed at 37˚C. The data were analyzed offline using pClamp 9.2 software (Molecular Devices).

SUPPLEMENTARY RESULTS AND DISCUSSION

Electrophysiology Results

To complement the Ca^{++}-imaging results of increased Ca^{++}-activation of $TRPV4_{P19S}$ in BEAS-2B airway epithelia, and similar Ca^{++}-signals in N2A neuronal cells, electrophysiolgical recordings from N2A cells were performed.

TRPV4 channel activity was induced by Ca^{++}-activation (2mM Ca^{++}) (Strotmann et al. 2003; Strotmann et al. 2010), which could be completely blocked using 10µM GSK205. Electrophysiological recordings revealed a functional gain in current responses for $TRPV4_{P19S}$. Both $TRPV4_{WT}$ and $TRPV4_{P19S}$ showed an outward rectification typical for TRPV4 channels. Current densities at +110 mV increased significantly for $TRPV4_{P19S}$ by approximately 30%.

Additionally relevant discussions re Ca^{++}-influx into airway epithelia

TRPV4 is possibly not the only critical Ca^{++}-conductance, pointing towards a role for other TRP channels that can form a heteromer together with TRPV4, or TRP channels that function together with TRPV4 in the same signaling cascade. Beyond TRP channels, other Ca^{++}-permeable channels could be involved as well, such as voltage-activated Ca^{++}-channels, known to be expressed in respiratory epithelia. – Addressing these questions will be the subject of stimulating future studies.

SUPPLEMENTARY MATERIAL, FIGURES 1-6

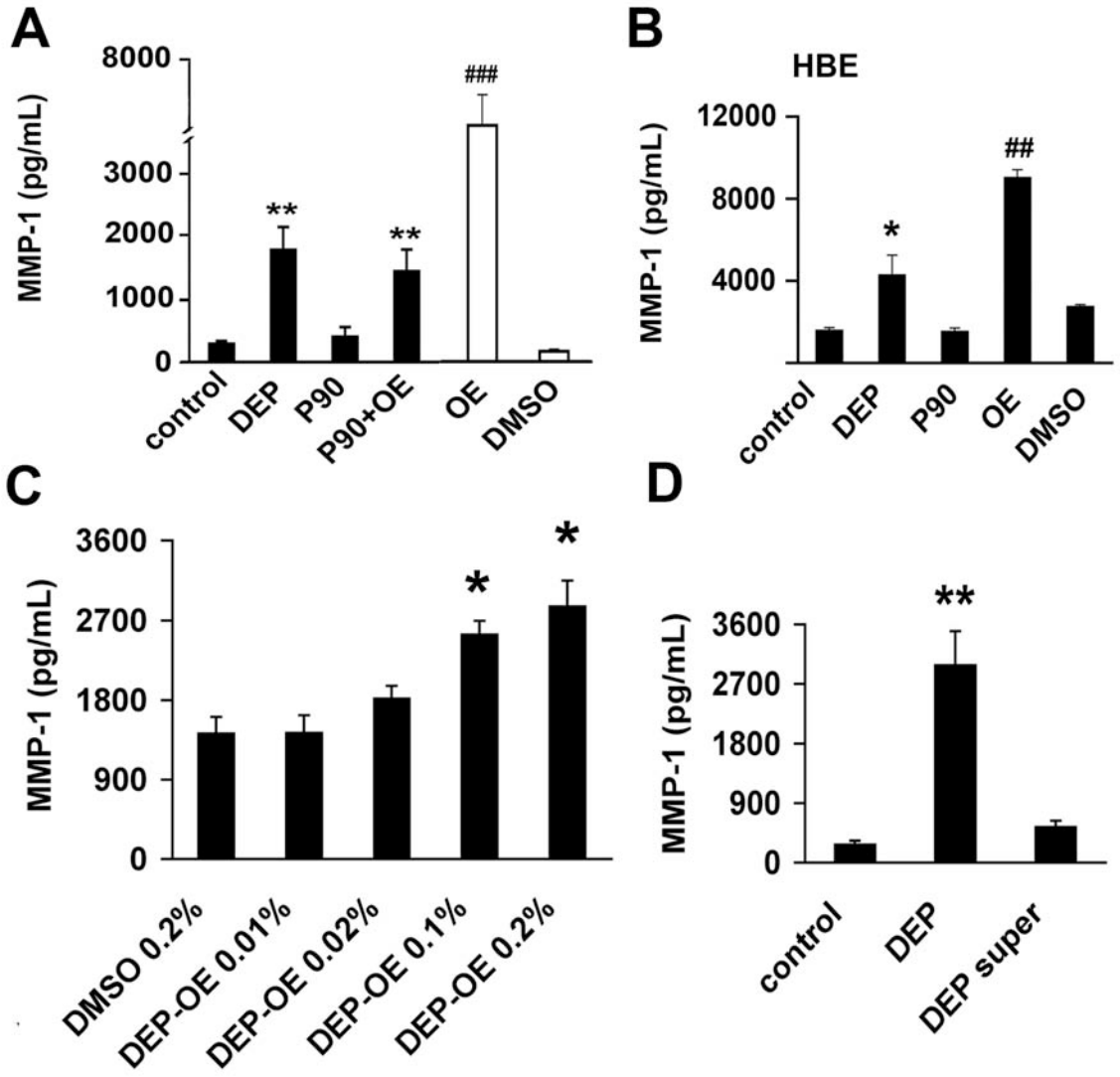

Supplementary Material, Fig. 1: DEP organic extract is the active principle for activation of *MMP-1.* A: This bar-diagram shows the effect of DEP on MMP-1 secretion in BEAS-2B cells, potentiation of the effect of DEP when using organic extract (OE) from the same particles, titrated to match 100µg/mL, plus reconstitution of the effect of DEP when using control carbon nanoparticles, P90, themselves inert, loaded with OE. Note lack of effect of vehicle control (0.2% DMSO) for OE. B: As in A, for primary human HBE cells. C: Dose-response relationship of MMP-1 secretion, measured by ELISA, for primary HBE cells exposed to increasing doses of OE. 20µg/mL OE in 0.2% DMSO correlates to 100µg/mL DEP. D: Virtual lack of activity of water-soluble DEP extracts on MMP-1 secretion, as measured by ELISA, using BEAS-2B cells.

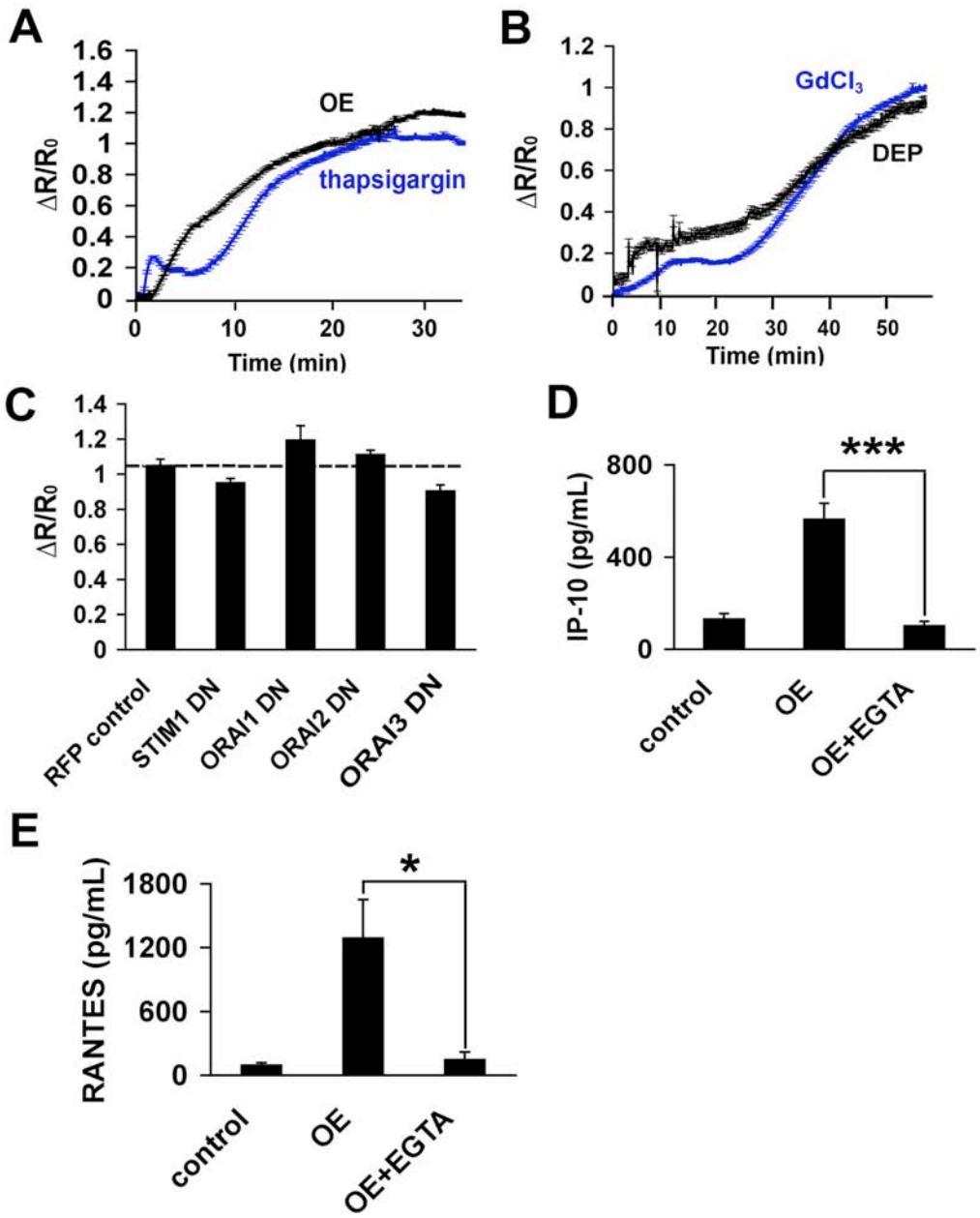

Supplementary Material, Fig. 2: DEP-evoked Ca^{++} effector mechanisms involving secretion of chemokines IP-10 and RANTES, independence from intracellular Ca^{++} stores. All experiments shown in this figure were obtained with BEAS-2B cells.

A: Emptying intracellular stores with thapsigargin (5μM) does not affect Ca^{++}-entry in response to OE. B: Inhibition of the store-operated Ca^{++}-entry (SOCE) mechanism, using 5μM $GdCl_3$, does not affect Ca^{++}-entry in response to DEP. C: Inhibition of molecules implicated in SOCE mechanisms, STIM1, ORAI1-3, by transfection of their dominant-negative (DN) isoforms, does not affect Ca^{++}-entry in response to OE; note that all constructs were fused to GFP, Ca^{++}-imaging only conducted in GFP^{+} cells. Shown is the averaged $\Delta R/R_0$ at 20'. D: IP-10 secretion, measured by ELISA, is significantly increased in response to DEP-OE-exposure, using BEAS-2B cells. Note the elimination of its secretion when conducting the assay in the absence of extracellular Ca^{++}. E: As in D, shown here are results for RANTES.

Supplementary Material, Figure 3

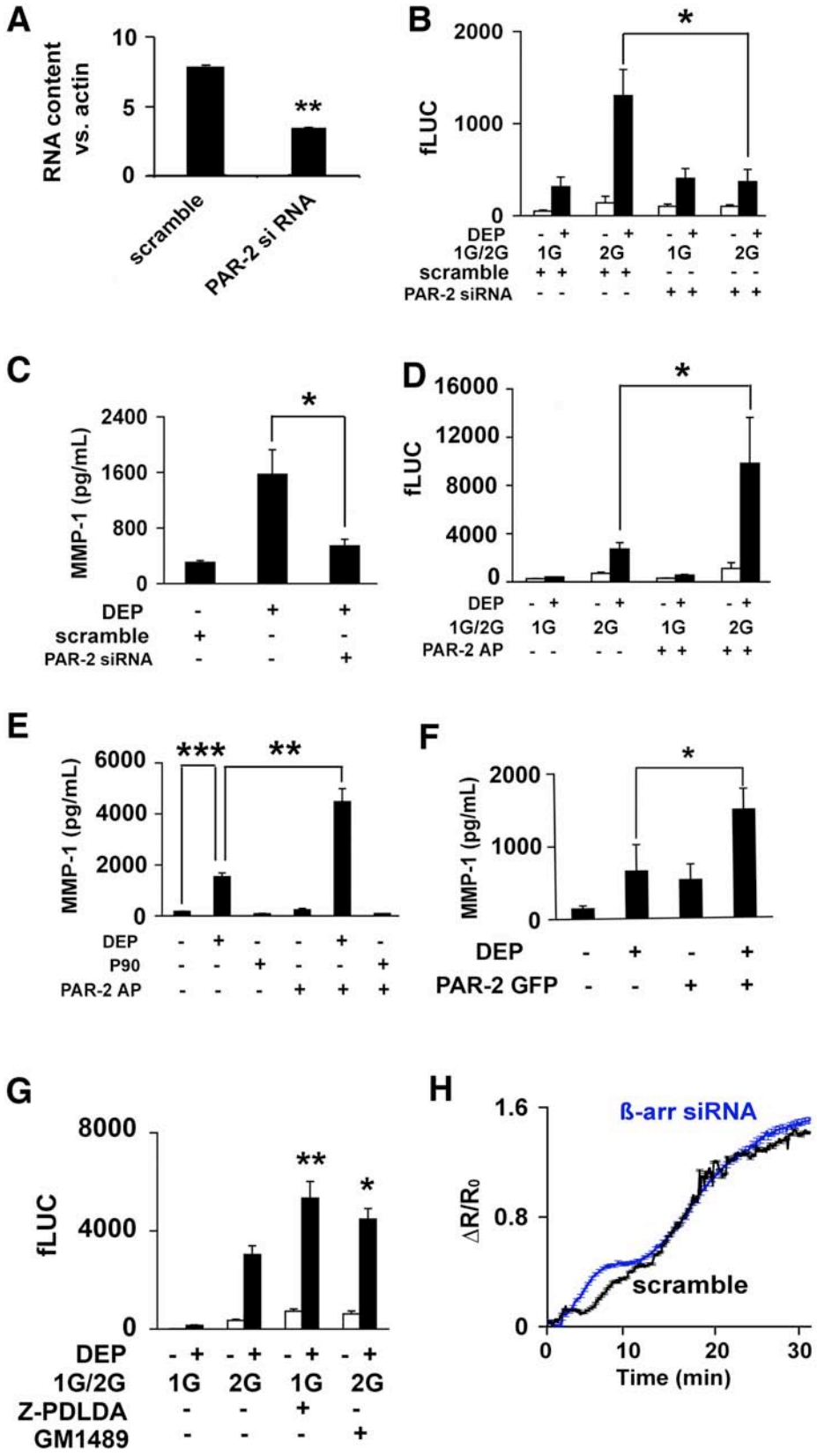

Supplementary Material, Fig. 3: PAR-2 is necessary for DEP to activate MMP-1; co-activation of PAR-2 potentiates DEP's effect on MMP-1. All results depicted here were obtained using BEAS-2B cells. A: This bar diagram shows the efficiency of siRNA-mediated PAR-2 knock-down, note significant reduction of normalized PAR-2 mRNA, detected by Taqman qRT-PCR comparing PAR-2 specific siRNA vs. scrambled controls. B: This bar diagram shows transcriptional activation of *MMP-1* in response to DEP, and its elimination, for the -1607GG *MMP-1* polymorphism, upon transfection of PAR-2 specific siRNA molecules. C: Depicted here is the robust reduction of MMP-1 secretion in response to DEP upon transfection of PAR-2 specific siRNA vs. scrambled controls. D: This diagram illustrates the potentiation of DEP-evoked *MMP-1* transcriptional activation by activation of PAR-2, using *MMP-1* reporter genes, for both -1607G and -1607GG *MMP-1* polymorphisms. Note the insignificant increase in *MMP-1* reporter activity, for the 2G polymorphism, when exclusively activating PAR-2, and the robust increase upon DEP exposure, in contrast to the striking increase when exposing cells to both, DEP plus PAR-2-AP. E: This diagram illustrates the potentiation of the effects of DEP by PAR-2 activation on MMP-1 secretion. Note the complete lack of effect when using P90 as control particle, either by itself or in combination with PAR-2-AP. Also note MMP-1 production reaching robust amounts for DEP stimulation alone, and striking amounts for DEP plus PAR-2-AP. F: This diagram shows the results of another method for accomplishing PAR-2 gain-of-function, namely by transfection of extraneous receptors. This leads to a potentiation of MMP-1 secretion by transfected BEAS-2B cells. Note the moderate increase in MMP-1 secretion for PAR-2-GFP without DEP exposure vs. the potentiation for PAR-2-GFP transfected cells that were exposed to DEP vs. DEP exposure of cells with endogenous levels of PAR-2. G: Depicted here is *MMP-1* reporter gene activity (24h time-point) in response to DEP, and the significant increase that we recorded upon pre-incubation of potent pan-MMP-inhibitors, Z-PDLDA and GM1489. These data are not compatible with a feed-forward mechanism of secreted MMP-1 (or any other secreted MMP) cleaving and activating PAR-2. H: This Ca^{++} time-course indicates no difference between cells subjected to pan-ß-arrestin knockdown/knockout, via specific siRNA, and scrambled siRNA transfected cells. This lack of difference suggests that ß-arrestins do not function critically up-stream of Ca^{++}-influx, e.g. in regulating PAR-2.

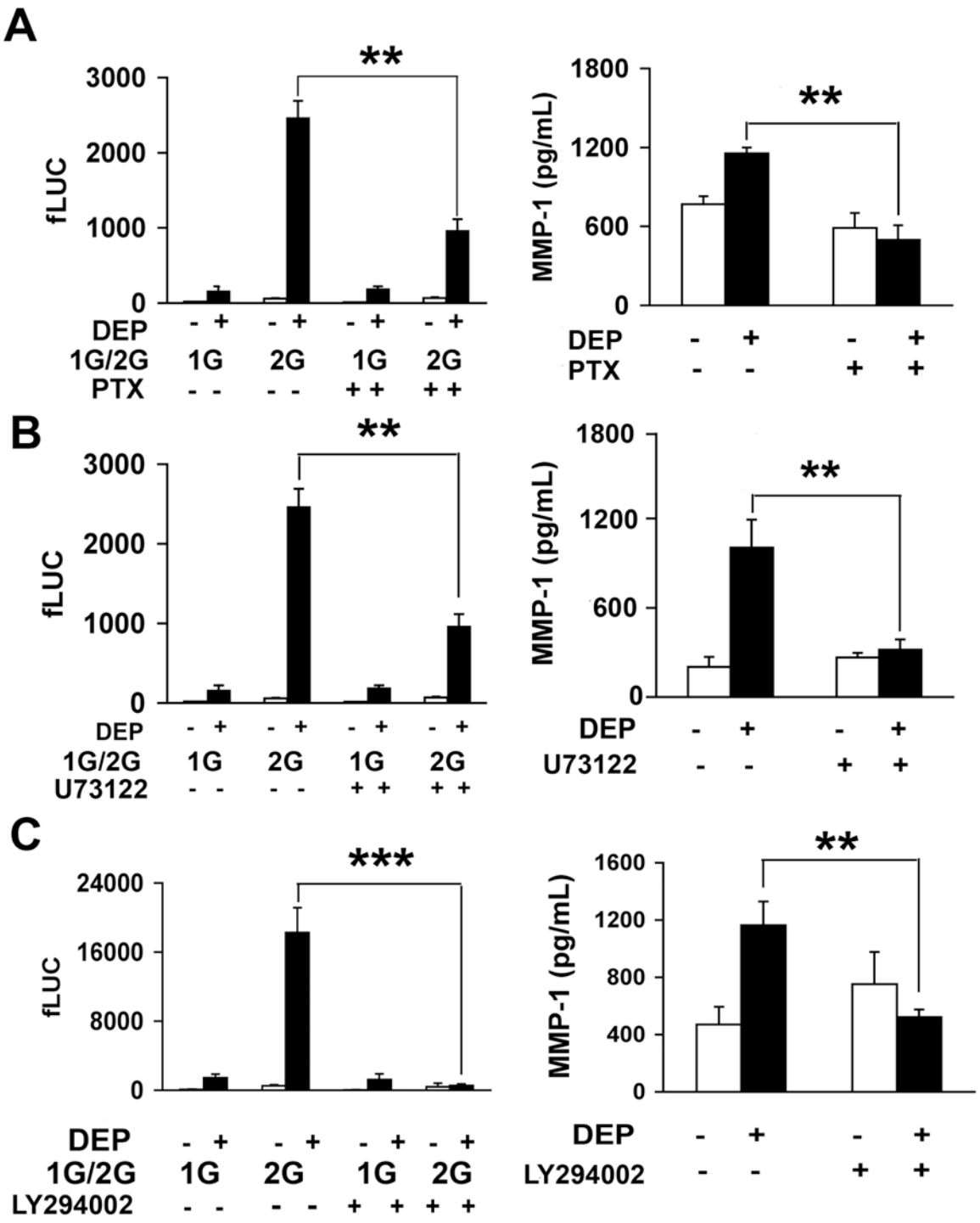

Supplementary Material, Fig. 4: $G_{i/o}$, PLC and PI3K are needed for DEP to activate MMP-1. Left-hand bar diagrams show *MMP-1* reporter gene activity in response to DEP, for both *MMP-1* polymorphisms, -1607G (1G) and -1607GG (2G), in BEAS-2B cell. Right-hand diagrams show DEP-exposure evoking MMP-1 secretion from BEAS-2B cells. A: Specific inhibition of $G_{i/o}$ with pertussis toxin (PTX) indicates a critical role for this G-protein. B: Inhibition of PLC-activity with U73122 indicates a critical role for PLC. C: Inhibition of PI3-kinase activity with LY294002 indicates a critical role for PI3-kinase.

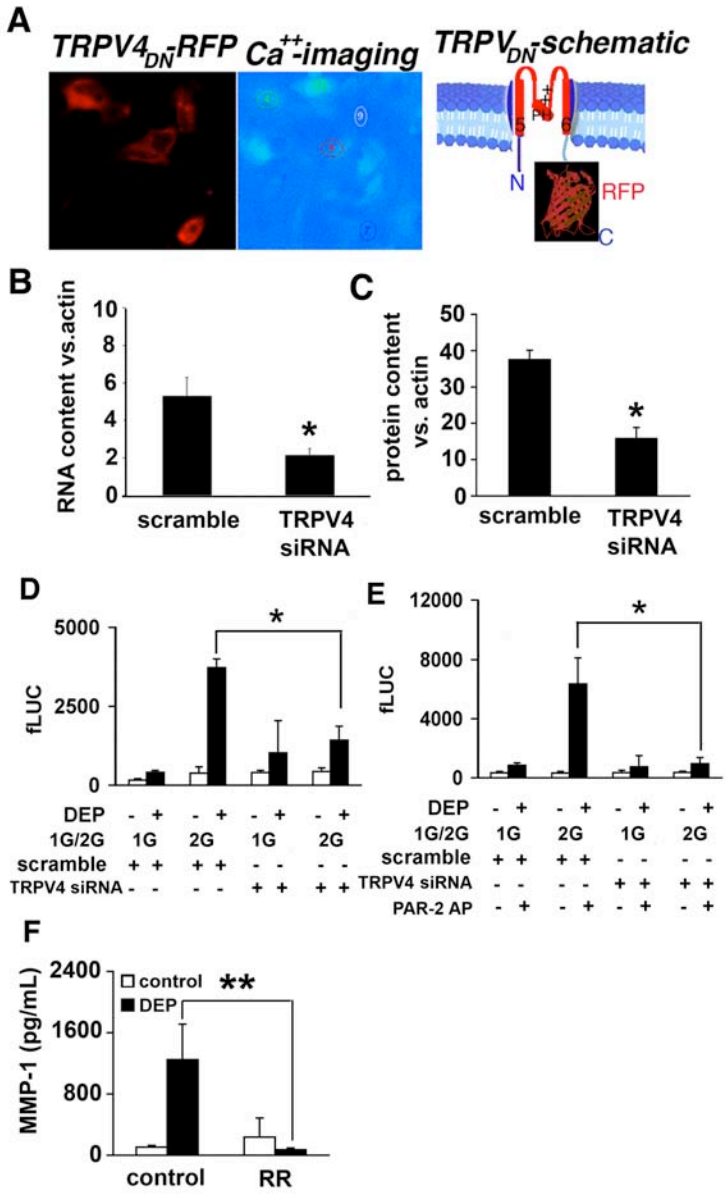

Supplementary Material, Fig. 5: TRPV4-related findings. All experiments conducted in BEAS-2B cells. A: The left-hand micrographs show RFP-fused DN-TRPV4 expression in transfected BEAS-2B cells, and its effect on Ca^{++}-transients (ratiometric pseudoimage, micrograph in the middle). The right hand schematic depicts the principle of the TRPV-DN isoforms, namely truncation before TM5 and after TM6, C-terminal fusion to RFP and engineering of a double-positive charge into the respective selectivity filter. B: This bar diagram depicts specific down-regulation of TRPV4 gene expression, as measured by Taqman qRT-PCR, by specific siRNA transfection. C: This bar diagram depicts specific down-regulation of TRPV4 protein expression by specific siRNA transfection. D: *MMP-1* transcriptional activation in response to OE depends on TRPV4 (BEAS-2B cells). TRPV4 siRNA significantly reduced transcriptional activation for the 2G-polymorphism, note absence of effect with scrambled control. E: TRPV4 functions down-stream of PAR-2 in response to DEP/OE. Similar to (C), yet notice co-stimulation of PAR-2 when exposing cells to DEP potentiates the response. Note the complete elimination of the potentiation of cells' response to DEP plus PAR-2-AP when knocking down TRPV4 with specific siRNA. F: Depicted is MMP-1 secretion in response to DEP, completely eliminated by TRP(V) inhibitor ruthenium-red (10µM preincubation; BEAS-2B cells).

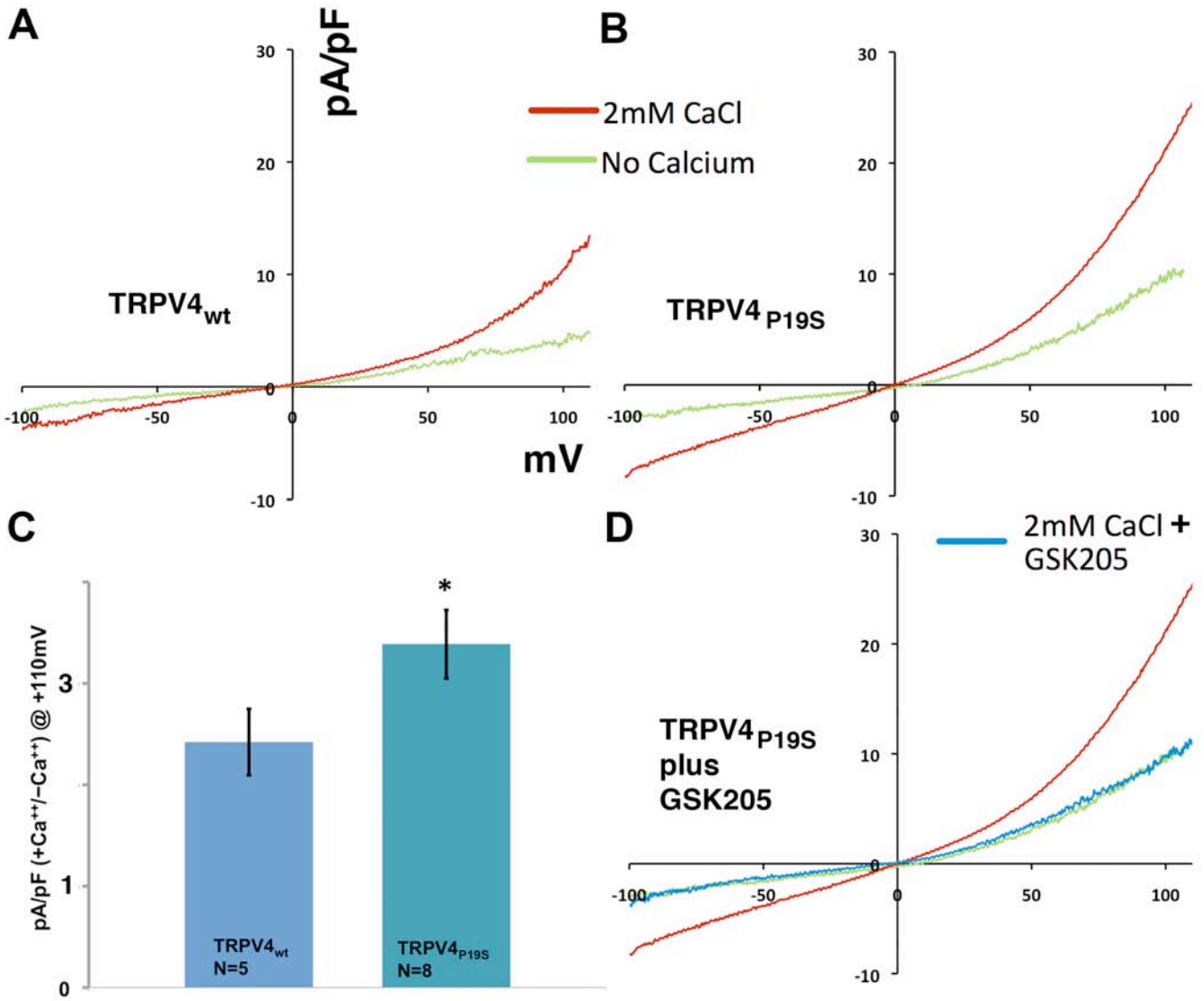

Supplementary Material, Fig. 6: Patch-clamp recordings of $TRPV4_{P19S}$, heterologously expressed in N2A cells. Currents were obtained from voltage ramps applied from -100 mV to +110 mV in N2A cells. A: A representative I-V trace of Ca^{++}-activated $TRPV4_{WT}$ channels expressed. B: The electrophysiological responses of Ca^{++}-activated $TRPV4_{P19S}$ channels are depicted here. C: Shown are Ca^{++}-activated mean current densities. The ordinate of pA/pF at +110mV represents a normalized ratio of pA/pF post-Ca^{++}-activation to pre-Ca^{++}-activation; data expressed as mean ± SEM (* $p < 0.05$, t-test; n = as indicated). D: Both $TRPV4_{WT}$ (not shown) and $TRPV4_{P19S}$ channel activity in response to Ca^{++}-activation (shown here) were completely blocked with 10µM GSK205, so that the respective trace superimposes with the pre-Ca^{++}-activation.

Supplementary References

Ghio AJ, Cohen MD. 2005. Disruption of iron homeostasis as a mechanism of biologic effect by ambient air pollution particles. Inhalation toxicology 17(13): 709-716.

Gilmour MI, McGee J, Duvall RM, Dailey L, Daniels M, Boykin E, et al. 2007. Comparative toxicity of size-fractionated airborne particulate matter obtained from different cities in the United States. Inhalation toxicology 19 Suppl 1: 7-16.

Li J, Ghio AJ, Cho SH, Brinckerhoff CE, Simon SA, Liedtke W. 2009. Diesel exhaust particles activate the matrix-metalloproteinase-1 gene in human bronchial epithelia in a beta-arrestin-dependent manner via activation of RAS. Environ Health Perspect 117(3): 400-409.

Perez CA, Huang L, Rong M, Kozak JA, Preuss AK, Zhang H, et al. 2002. A transient receptor potential channel expressed in taste receptor cells. Nat Neurosci 5(11): 1169-1176.

Phan MN, Leddy HA, Votta BJ, Kumar S, Levy DS, Lipshutz DB, et al. 2009. Functional characterization of TRPV4 as an osmotically sensitive ion channel in porcine articular chondrocytes. Arthritis and rheumatism 60(10): 3028-3037.

Strotmann R, Schultz G, Plant TD. 2003. Ca2+-dependent potentiation of the nonselective cation channel TRPV4 is mediated by a C-terminal calmodulin binding site. J Biol Chem 278(29): 26541-26549.

Strotmann R, Semtner M, Kepura F, Plant TD, Schoneberg T. 2010. Interdomain interactions control Ca2+-dependent potentiation in the cation channel TRPV4. PloS one 5(5): e10580.

Yasuda R, Nimchinsky EA, Scheuss V, Pologruto TA, Oertner TG, Sabatini BL, et al. 2004. Imaging calcium concentration dynamics in small neuronal compartments. Sci STKE 2004(219): pl5.